Emergent Materials (2021) 4:655–672
https://doi.org/10.1007/s42247-021-00204-7

REVIEW

MXenes and their composites for hybrid capacitors and supercapacitors: a critical review

Manavalan Vijayakumar[1,2] · George Elsa[2] · Aamani Nirogi[2] · Rajendran Navaneethan[2] · Ammaiyappan Bharathi Sankar[3] · Mani Karthik[2]

Received: 6 February 2021 / Accepted: 3 March 2021 / Published online: 13 March 2021

Abstract

MXenes are realized as an innovative family of two-dimensional (2D) structured materials resembling the structure like graphene and molybdenum disulfide. The extensive research has been explored in this novel family of MXene materials from the discovery of Ti_3C_2 in 2011. Around 20 variants of MXenes have been synthesized, and the structural properties of more than dozens of MXene materials have been theoretically predicted. Unlike other 2D ceramics, MXenes have excellent electrical conductivity and exceptional efficiency since they are molecular sheets composed of carbide and transition nitride metals such as titanium. MXenes are formed by etching a coating from MAX phases and adding the suffix "ene" to highlight their resemblance to graphene. MAX phases are a family of hexagonal faceted ternary transition metal carbides, carbonitrides, and nitrides composed of $M_{n+1}AX_n$, where *M* represents for transition metals (such as Cr, Nb, Ti, V), *A* indicates group of A elements (such as In, Al, Si, Sn), *X* means carbon and/or nitrogen, and *n*=1, 2, or 3. MXenes have already established numerous applications such as energy storage, modular electronics, optoelectronics, medicine, and nano-biosensors. In this review article, the synthesis technique, configuration, and electronic properties of MXenes are emphasized and extensively discussed. MXenes and MXene-based nanocomposites for electrical energy storage applications are mainly highlighted and outlined. Finally, MXene-based hybrid supercapacitors as next-generation energy storage devices are summarized and briefly discussed.

1 Introduction

1.1 Concept of energy storage and technology

Sustainable and renewable energy conversion technologies and their development have become the consensus of scientists all over the world. Renewable sources of energy like wind, solar, and tidal can minimize the usage of fossil fuels and reduces the greenhouse gas emissions in power generation [1]. Solar photovoltaic (PV) and wind energy conversion technologies exhibit variable power supply and ambiguous output. Renewable energy sources like wind and sun are uncertain energy sources because the wind does not blow continuously, and the sun does not shine constantly at any given location [2]. There is an urgent need to create a relatively constant energy storage device as a crucial component for future powering systems. In the future, the electricity grid has to include energy storage systems to maintain the uninterrupted power supply to the end consumers [3].

The power grid is a complex mechanism in which the power generation and power demand should be balanced at any given time. The constant supply modifications are needed for predictable power demand shifts, such as normal trends of human activity, as well as unpredictable incidents from overloads of the high-power demand of alternators [4]. Energy storage plays an imperative role in the balancing act which also facilitates the development of more sustainable and secure grid infrastructure. For example, where there is more energy availability than power consumption during the night when low-cost power stations start running, surplus electricity generation for reserved capacity could be used. When the power demand exceeds supply, storage facilities will

✉ Mani Karthik
mkarthik@project.arci.res.in; karthik_annauni@yahoo.co.in

[1] Global Innovative Centre for Advanced Nanomaterials (GICAN), Collage of Science, Engineering and Environment, The University of Newcastle, NSW 2308 Callaghan, Australia

[2] Centre for Nanomaterials, International Advanced Research Centre for Powder Metallurgy and New Materials (ARCI), Balapur, Hyderabad 500005, India

[3] School of Electronics Engineering, Vellore Institute of Technology (VIT), Chennai Campus, Chennai 600127, India

distribute their stored energy to the reservoir. Energy storage is awaited to play a huge role in the coming century, with more storage capacity solutions evolving and the transition from the planet to a cleaner energy economy. Energy storage is also used as a fast solution, and most storage systems will start to discharge electricity into the grid very rapidly, whereas fossil fuel supplies appear to ramp up longer. This rapid response is critical to ensure grid reliability when unanticipated demand changes occur [5].

While considering environmental climate changes and economic standards, it is important to examine different competing technologies including generation, transmission, distribution, and operational circumstances. To store energy for a long period, different energy storage technologies are available in the market such as batteries, supercapacitors (SCs), thermoelectric, mechanical storage, hydrogen, and pumped hydropower [6]. Based on the technology and its application, design considerations and specific factors change for each component used in the application, i.e., reliability, environmental impact, and safety. Generally, various energy storage technologies have been developed and demonstrated as illustrated in Fig. 1. The electricity storage systems vary in shape and size depending on the type of energy stored which include thermoelectric, hydro, gas turbine, flywheel, superconductive magnetic coil, SC, lead-acid battery, Li-ion battery (LIB), and fuel cell stacks. To reduce the gap between power demand and availability of electricity, electrical energy storage systems tend to reduce scheduling variations [7].

Energy storage is a process that transforms one form of energy into another form by storing it and using the stored energy at a later time. Electrical energy can be derived from renewable energies, such as solar or wind, and has a major obligation to fulfill potential energy needs [8]. This technology will help to remold the energy sector by integrating renewable energy sources (solar power and wind) into the utility grid as shown in Fig. 2. It will allow saving the electrical energy by supporting the sudden power demand variations in balancing and maintaining the grid. Globally, there has been a shift towards clean energies with more focus on climate change, and there is a gradual transition from fossil fuels to renewable resources. Energy storage traditionally refers to storing electrical energy previously generated for use at a later time. Simultaneously, energy from renewable sources should be stored effectively and efficiently in energy storage devices.

Currently, LIBs contribute a predominant function particularly hybrid electric and various electronic gadgets. Rechargeable LIBs and SCs are the most beneficial inventions for electrochemical energy storage (EES) systems [9]. LIB batteries often carry huge energy densities but offer low power densities that limit their operation in an environment that demands more energy. SCs, on the other hand, offer higher power densities with outstanding cycling efficiency with low energy densities being their liability. As a result, many researchers around the world are researching new materials of excellent energy and power density and are therefore viable over a longer span of existence [10].

Since the finding of exfoliated graphene films in 2004, 2D material with a layered structure has appealed to a great research interest among scientists due to their fantastic electronic and structural properties. After the two decades of the successful mechanical exfoliation of graphene from three-dimensional (3D) graphite, several 2D nanomaterials have

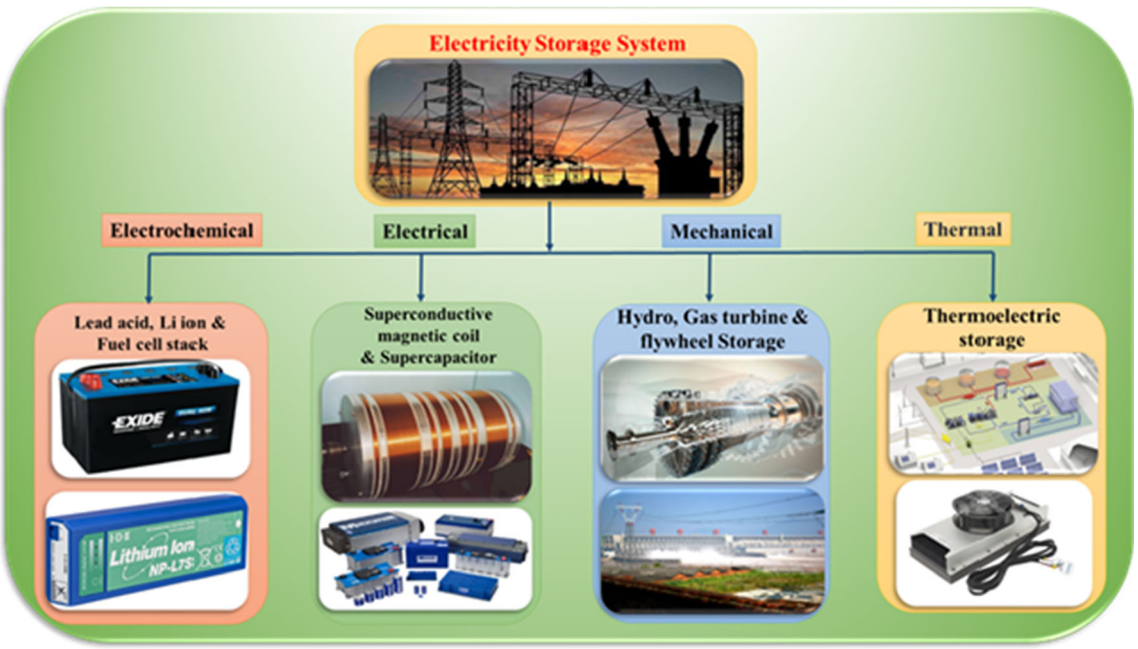

Fig. 1 Various technologies of an electricity storage system

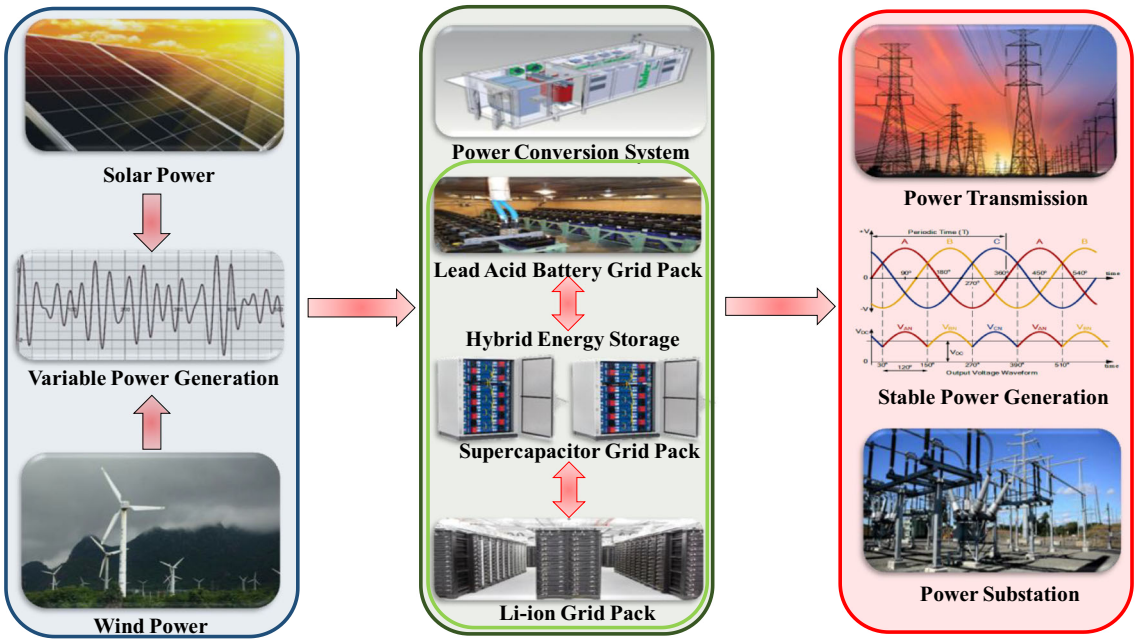

Fig. 2 Integration of renewable energy sources from solar power and wind power to the utility grid

been explored by using different preparation and exfoliation methods from different layered precursor materials which include metal-organic frameworks (MOFs), graphitic carbon nitride (g-C_3N_4), and different MAX phase (e.g., Ti_2AlC), as well as other precursors, which are utilized to obtain the 2D transition metal carbides (TMC), carbonitrides, and nitrides; those are generally called "MXene" [11].

2D materials could act as fundamental building blocks to form various layered structures, composites, and membranes. Even though some individual 2D elements, such as graphene, silicon, germanene, and phosphorene, are synthesized, most of these materials are comprised of two or more atoms, such as chalcogenides in metal transition and double-layered hydroxides [12]. Graphene has shown outstanding research potential in 2D materials and has immense energy conservation and transformation capacity. For the first time, Gogotsi's research group reported the convergence of metallic conductance and hydrophilic surfaces in a novel constellation of graphene-like 2D compounds, metal transition carbides, carbonitrides, and nitrides, and this category of 2D material was known as MXenes [13]. Following this discovery of the MXenes, several scholars have researched systematically the design and production of 2D materials because of their excellent electrical, optical, and mechanical characteristics, which have a high aspect ratio. Figure 3 indicates that the number of articles published is related to MXenes and MXenes composites [14].

In particular, MXenes have high electrical conductivity and outstanding performance as compared to other 2D materials, since they are molecular sheets crafted from carbides and transition metal nitrides such as titanium. These types of 2D layer-structured materials are known as "MXenes" since they generate a MAX layer of layer and incorporate a suffix called "ene," which underlines their graphene resemblance. The MAX phases are a huge group of ternary hexagonal layered transition metal carbides, carbonitrides, and nitrides with a chemical formula of $M_{n+1}AX_n$, where *M* is the transition metal like Ti, V, Cr, and Nb, where *A* indicates group A elements such as Al, Si, Sn, and In, *X* indicates carbon and/or nitrogen, and *n* indicated as *n*=1, 2, or 3 respectively. The MAX phase means a variety of metals with $M_{n+1}AX_n$ chemical composition. The present review article introduces and explores thoroughly the synthesis techniques, structural composition, and

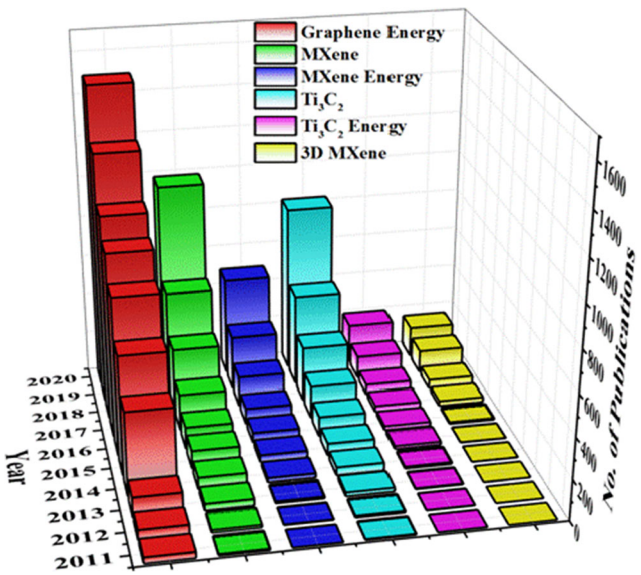

Fig. 3 The number of articles published each year in the field of MXenes and MXene-based composites.

physicochemical properties of MXenes. Special attention has been given to MXenes and their composite materials for energy storage applications. Finally, MXene-based hybrid SCs as next-generation energy storage devices are also extensively discussed.

2 Synthesis strategy of MXenes

After the identification of peculiar properties of graphene, there has been a substantial investigation on 2D materials. In this concern, 2D TMC and nitrides are explored, and it is called as MXenes (pronounced as "Maxenes") that was steadily increasing class of 2D materials. MXene is a novel type of organized 2D material which is similar to that of graphene and molybdenum disulfide material. This novel family of MXene has been thoroughly investigated in the year of 2011, after the discovery of Ti_3C_2 material. To date, there are around 20 variants of MXenes that have been synthesized, and their structural and physicochemical properties of more than dozens of MXenes have been theoretically predicted. Also, such materials find an extensive potential material in various applications. The history and evaluation of MXenes are schematically represented in Fig. 4.

MXene has a standard formula of $M_{n+1}X_nT_x$ where T_x indicates the surface circumcisions that are bound to the outer M layers (O, OH, F, and/or Cl). MAX phases have a hexagonal-layered configuration in which *M* layers are virtually closed, and octahedral sites are filled by *X* atoms. Layers of $M_{n+1}X_n$ are then interlaced with element A, which is metallically attached to element M. MXenes also have three different structures of one metal at the M-site, as obtained from the parent peak phases: M_2C, M_3C_2, and M_4C_3. They are generated by carefully inscribing the element A of the MAX process or other layered predecessor (e.g., Mo_2Ga_2C) with the structural formula of $M_{n+1}AX_n$, where *M* is an early transition metal, *A* is an element of the periodic table group 13 or 14, *X* is C and/or N, and n = 1–4. These are generally referred to as mono-transition metal MXenes. MXene carbides consisting of two transition metals referred to as double transition MXenes have also been synthesized [15].

In this latest millennium, MXenes have been standardized as $M'_2M''C_2$, $M'_2M''_2C_3$, or $M'_4M''C_4$. Mo_2TiC_2, $Mo_2Ti_2C_3$, Cr_2TiC_2, and Mo_4VC_4 contain synthesized double transition metal carbides, where M′ and M″ are different transition metals. Mo or Cr atoms are extreme parts of the MXene such as Mo_2TiC_2, $Mo_2Ti_2C_3$, and Cr_2TiC_2, and these atoms are responsible for the electrochemical efficiency of the MXenes, while in some of the MXenes like Mo_4VC_4 or $(Mo,V)_4C_3$, the metals are aimlessly dispersed across the system in stable solutions. Generally, MXenes are fabricated by using different techniques as schematically represented in Fig. 5.

For example, amine-assisted delamination is being a two-step process and frequently utilized to segregate different layered materials into 2D nanosheet materials [16], which are generally obtained through intercalation of an organic compound into the layered structure followed by sonicating in a solvent. Dimethyl sulfoxide (DMSO) can act as an intercalating agent during the synthesis of MXenes [17]. Initially, multi-layered $Ti_3C_2T_x$ flakes can be delaminated. Afterward, the delamination of this same compound could also be carried

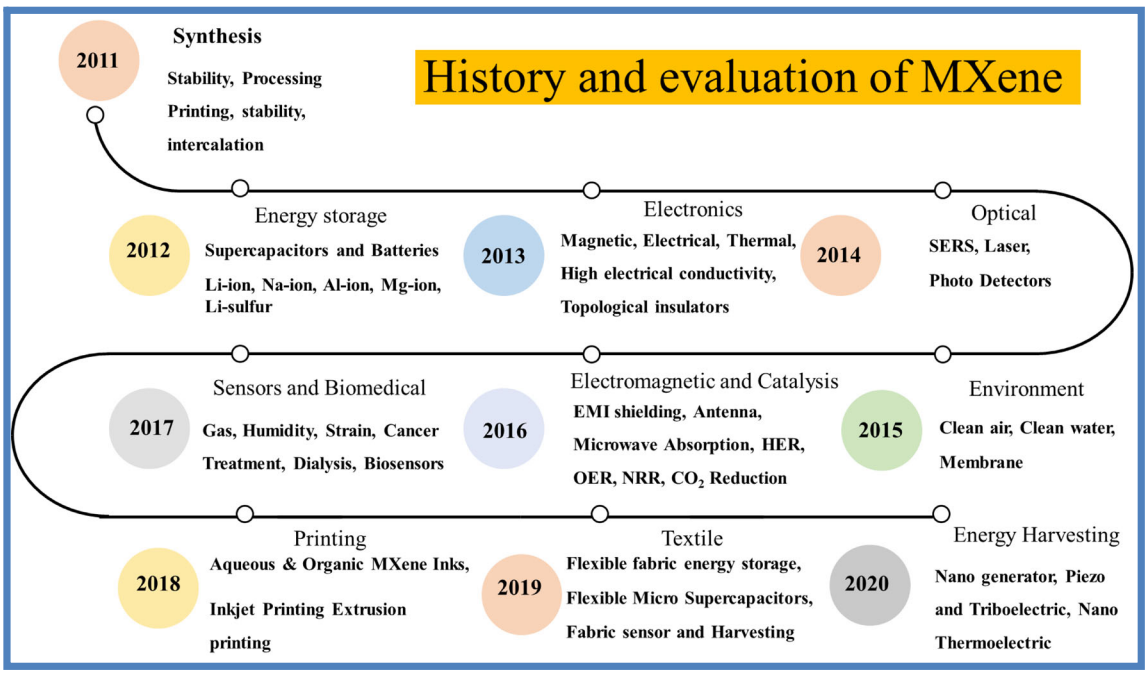

Fig. 4 History and periodic assessment of MXene and MXene-based composites for numerous potential applications

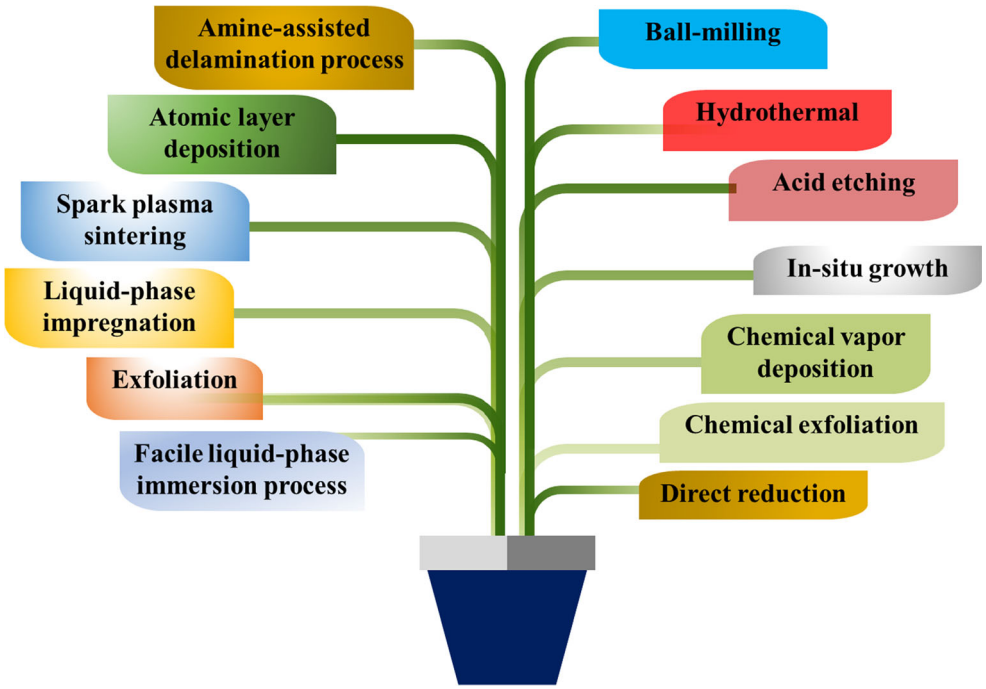

Fig. 5 Various routes for fabrication of MXenes

out by using a simple etching method of the MAX phase, Ti_3AlC_2, in a solution containing LiF and HCl [18]. On the other hand, the coating of SnO_2 and HfO_2 with ALD (atomic layer deposition) was specifically applied to MXene layers coated on a Cu surface. MXene base can be prepared by using the mixer of MXene powder, acetylene black, and polyvinylidene fluoride (PVDF) with a corresponding weight ratio of 80:10:10 by adding NMP as a solvent for preparing the homogenous mixture. By using a doctor blade instrument, the prepared mixture was evenly transposed on a copper foil having a coating thickness of 100μm, and the coated material was dried at a temperature of 80°C for 24 h under vacuum condition. For SnO_2 and HfO_2 deposition, the MXene-coated Cu foil was placed into the atomic layer deposition chamber with the measurement of material active mass (1–2 mg cm^{-2}). For example, SnO_2 was deposited at two different temperatures of around 150°C and 200°C by using an ALD reactor. The deposited sample at 150°C was further treated in subsequent steps: (i) a constant N_2 dose at 20 psi, (ii) a dose of Sn precursor (Tetrakis (diethylamide) tin (IV)) at 0.5s, (iii) an Sn precursor reaction time of 30 s, (iv) an O_3 oxidant dose at 0.2 s, and (v) an oxidant reaction time of 15 s with a deposition rate of 0.1 nm per stage. The standard cycle at 200°C contained the same precursors, but the reaction times were modified to achieve a reasonable thickness of SnO_2 MXene sheets.

On the other hand, ultra-thin films of HfO_2 were also deposited at 180°C on the surface of the SnO_2/MXene electrodes. The following steps are involved in the preparation of HfO_2 deposition by using the ALD technique: (i) a constant 20 psi N_2 dose, (ii) a 0.015 s H_2O dose, (iii) a 10 s H_2O reaction time, (iv) a 0.2 s Tetrakis (dimethylamino) hafnium ($Hf(NMe_2)_4$) precursor dose, and (v) a 15 s $Hf(NMe_2)_4$ reaction time with a growth rate of 0.1 nm per cycle [18]. ALD was utilized to implant one single layer of metal carbide (MXene) onto mTMDC (single-layer transition metal dichalcogenide) and to eventually oxidize the top layer of metal atoms [19]. Spark plasma sintering (SPS) is one of the promising methods owing to its numerous benefits offered over other MAX-phase preparation techniques. The PL-SPS densification process is similar to the conventional SPS method, and the transport mechanism is similar to the grain size diffusion. The mechanical compaction is used only relevant to the punches that cause the grain to move the current and the reaction merging into the grain boundary instead of the friction. The spark current flows to punches and finally to the sample that is sintered through the electrodes [20]. It is a unique process used to accumulate pressurized powder in which pulsed direct electrical current travel through the sample and it is pushed through a matrix of graphite. The electric current sintering is also referred to as the ground-assisted or pulse-assisted sintering process [21]. The loaded solution is then mixed with the sample, and the solvent is evaporated in a liquid-phase impregnation process. An impregnation by a formulation with a power sample is equal to the material's pore volume, and also it is added to the inception of the impregnation processes [22]. The process of exfoliation applies to the preparation of MXene from the MAX stage (discriminatory layers of A-group components in the MAX step using HF etchant solution) [23, 24].

The synthesis of MXene materials by ball-milling with the aid of liquid surfactants or solid microdermabrasion additives

is a result of high energy colliding nanosized particulates in balls-milling materials (bulk precursors). The transition of metal atoms into the perovskite (host) lattice was achieved upon the preparation under the oxidizing atmospheres, and the nano-sized metallic particles on the surface under reduced atmosphere conditions have been prepared by using an in situ growth approach [25]. Chemical vapor deposition (CVD) is another well-known process where the substrate is subjected to one or more unexpected reactants that react and decay on the surface of the substrate to produce the required thin film deposition [26].

MXenes are usually synthesized by a top-down systematic etching technique as depicted in Fig. 6. This synthesis technique is considered a versatile technique because there is no degradation or alteration of the properties of the material when the batch size is increased. The processing of MXene through etching the MAX step occurs primarily by the use of solid etching solutions containing fluoride ions (F^-) such as HF, NH_4HF_2, and a blend of HCl and LiF. For example, $Ti_3C_2T_x$ MXene is fabricated by randomly etching the Ti_3AlC_2 (MAX) layers by using HF and LiF/HCl [27]. Ti_4N_3 MXene was first identified as the MXene nitride, and it is synthesized from MXene carbide using a separation process. To synthesize Ti_4N_3, the MAX step Ti_4AlN_3 is combined with the combination of liquid eutectic fluoride salt such as lithium fluoride, sodium fluoride, and potassium fluoride operated at high temperatures. This process is based on Al, which generates multilayer Ti_4N_3 that could be delaminated further into single and few layers by dipping MXene in tetra butyl ammonium hydroxide followed by sonication process [28].

This process involves mounting and removing surface functional groups by replacing and reducing reactions of molten inorganic salts [29]. Since MXenes are compact, the guest molecules in MXenes can be easily intercalated. Dimethyl sulfoxide, hydrazine, and urea can act as guest molecules. For instance, N_2H_4 (hydrazine), which is analogous to the basal MXene plane, can be intercalated to form a monolayer into $Ti_3C_2(OH)_2$. The intercalation strengthens the lattice parameter of MXene c (a parameter of a crystal structure linearly correlated to the distance between certain MXene layers) that decreases the connection between MX ion layers, and ion such as Li^+, Pb^{2+}, and Al^{3+}can also be intercalated with MXenes [30].

DMSO can also be used as an intercalation agent, and it is intercalated into powders of ML-MXene to aggressively extract the interlayer binding and then followed by the ultrasound therapy (Sonication) to obtain the $Ti_3C_2T_x$ nanosheets [29, 31, 32], and the process is represented in Fig. 7.

3 Physiochemical properties of various MXenes

MXenes are having an excellent electrical and mechanical properties. The hydrophilic surfaces of the MXenes are ready to bond with different species and show high negative zeta potential also allowing to form a stable colloidal solution in water, which makes an effective electromagnetic waves absorption contributes to a huge volume of electromagnetic waves. The various properties of MXene are represented in Fig. 8. However, the electronic and structural reported values

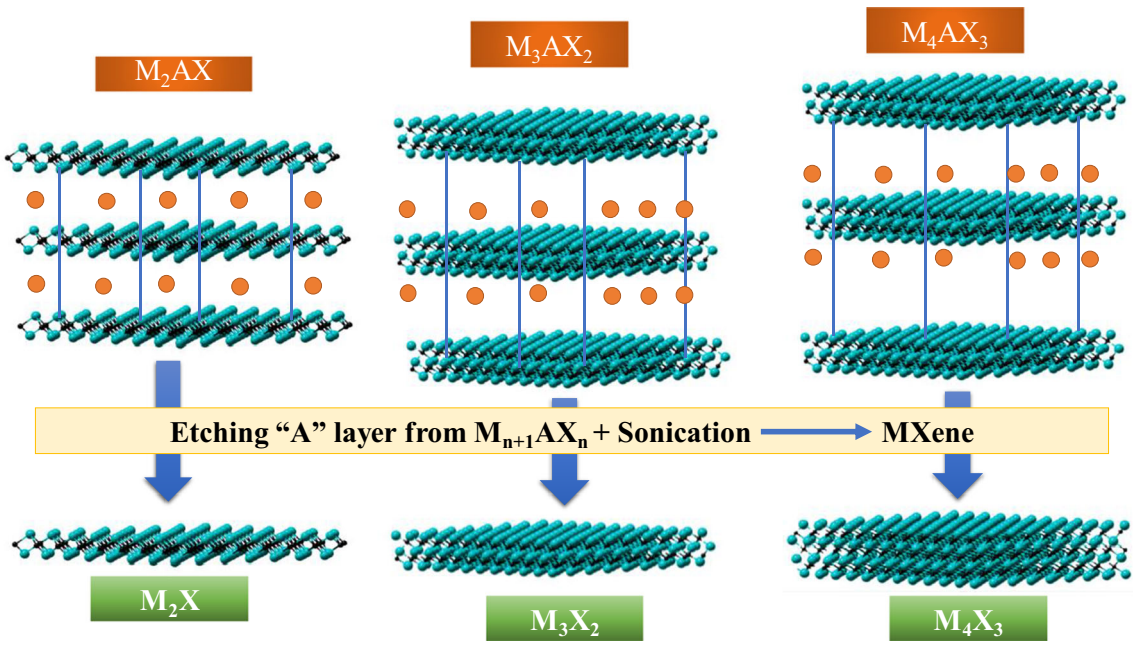

Fig. 6 Synthesis of MXenes by a top-down selective etching process

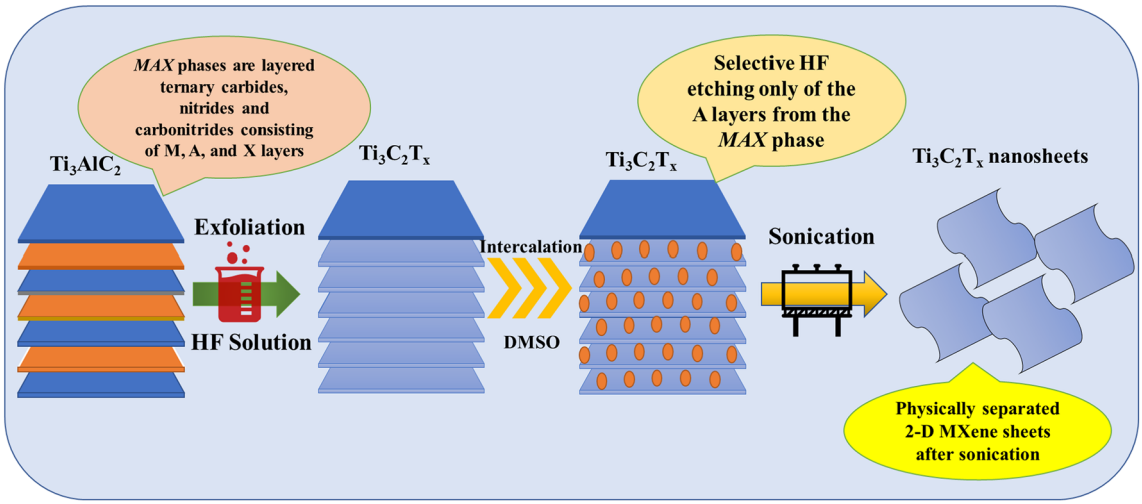

Fig. 7 Preparation of MXenes by intercalation method

are mostly theoretical, and very few experimental publications were reported in the ferromagnetism or topological insulators [33].

In general, MXenes without surface termination is supposed to be magnetic. However, MXenes like Cr_2C, Cr_2N, and Ta_3C_2 are predicted to be ferromagnetic, and on the other hand, Ti_3C_2 and Ti_3N_2 MXenes are anti-ferromagnetic. Monolayers of MXene are forecasted to be metallic material because there is a high electron density at the Fermi level. The bandgap of MXene is depending on the surface chemistry of MXenes [34–36]. However, the magnetic properties of the MXenes have yet been experimentally confirmed.

Since 2011, 20 different types of MXenes were synthesized. Each of them has excellent properties and a well-defined structure. Furthermore, they are theoretically defined well. MXenes are having a magnificent property because of its structure. The carrier mobility of MXene is around ~74100 and ~22500 $cm^2 V^{-1} s^{-1}$ along with different directions with a bandgap of 0.05 to 2.87 eV in the case of $Mo_2TiC_2(OH)_2$ and Sc_2CO_2 MXene. Sc_2CF_2 MXene with 50 µm flake length is having an electrical conductivity of around 9880 S cm^{-1} and thermal conductivity of 722 $Wm^{-1} K^{-1}$, respectively. Mechanical properties of MXenes are also noticeable with the results; the Young's modulus (502 GP in-plane) and tensile strength are around 8.2 MPa for $Ti_3C_2T_x$ material. The optical conductivity lies in the middle of the visible light spectrum with 40% of the variation for the $Ti_3C_2T_x$ MXene. The work function of Nb_2CT_x MXene is around 4.1 eV [37].

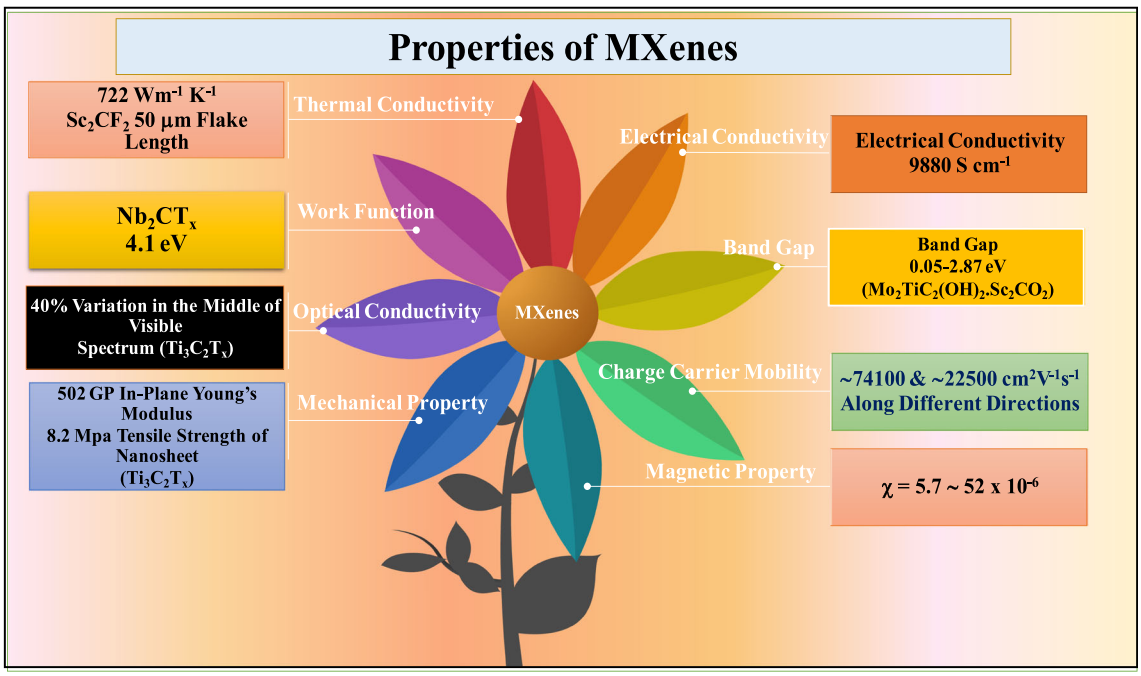

Fig. 8 Excellent properties of MXenes

Figure 9 depicts the electrical conductivities of MXenes before and after annealing conditions. The measured conductivity of Mo_2CT_x before annealing is approximately around 0.80 S cm^{-2}, which is increased to 1.2 S cm^{-2} by the end of the annealing process. However, the electrical conductivity of $Mo_2TiC_2T_x$ MXene will enhance twice the magnitude after curing the MXene material at 120°C for 18 h under vacuum conditions [38, 39]. The conductivity of pristine $Mo_2TiC_2T_x$ and $Mo_2Ti_2C_3T_x$ MXene is measured to be 44 S cm^{-1} (1494 S cm^{-1}) and 15 S cm^{-1} (614 S cm^{-1}), respectively [40]. After the first annealing cycle, the conductivity of MXene and Seebeck effect will stabilize, in such a case the material Mo_2CT_x and $Mo_2TiC_2T_x$ will act as metal, besides $Mo_2Ti_2C_3T_x$ material shows a semiconductor property, and it is purely depending on a majorly used MXene ($Ti_3C_2T_x$) which is having abundant specific capacity due to the prolific pseudo capacitive sites in it [41]. Upon analysis, the maximum theoretical capacity of $Ti_3C_2T_x$ material is around ~ 615 C g^{-1} in −0.6–0 V; furthermore, the experimental results also show 135 C g^{-1} in 0.55 V [42] but is very much lesser than the theoretical capacity. Although N -doped MXenes are fabricated by the solvothermal process, here nitrogen-doped $Ti_3C_2T_x$ is synthesized and got a high capacitance of around 2836 F cm^{-3} or 927 F g^{-1} at 5 mVs^{-1}, in 3M H_2SO_4 electrolyte, and it created a benchmark result for all the known MXenes. Also, MXenes are having a relevant electronic band structure. Its metallic behavior can be turned out by forming additional T-X bonds with the neighboring material. The MXene $Sc_2C(OH)_2$ is having a direct bandgap; however, the majority of MXenes have indirect band gaps [43, 44].

The greater electrical conductivity of MXene is due to its functionalization of material. If the film thickness is increased, the optical transmittance is decreased accordingly up to 86 %, and hence, the sheet resistance is also decreased to a value of 330 Ω sq^{-1}. A single nanosheet (~1.2-nm thickness) leads to a loss in transmittance of ~3%, which is common to that of graphene nanosheets (~2.3% loss per layer, 0.34 nm). The vacuum-filtered delaminated MXene sheet shows that the mechanical properties of a single- or two-layer nanosheet have proven to be quite challenging and also with the help of an atomic force microscope. The chip elastic properties of bilayer and monolayer $Ti_3C_2T_x$ were analyzed, and it was found to be 0.33 TPa [45]. The various properties of titanium carbide MXene ($Ti_3C_2T_x$) are shown in Fig. 10.

4 Energy storage application of MXenes and MXene-based nanocomposites

MXenes are very good electrical conductors and their surface termination can be easily tunable which plays an important role in energy storage applications. The synthesis feasibility of MXenes and their stability as colloidal suspensions in water along with its various organic solvents render will help in scaling up of MXene in large quantity. MXenes are highly known for their hydrophilicity and peek electrical conductivities, and the various properties of MXenes and their applications are shown in Fig. 11. From the figure, it is observed that MXene will be a promising material for energy storage applications, electromagnetic interference shielding, transparent conductive electrodes, etc.

Table 1 compares different synthesis approach to obtain MXene-based materials used in different energy storage application which include LIBs, SC, and hybrid capacitor. MXene-based LIB shows the capacity of 544 mAh g^{-1} @ 1.75 C rate for the material PVP-Sn(IV)-modified Ti_3C_2 synthesized using liquid-phase immersion procedure, and also other materials such as Nb_2CT_x/10%CNT (carbon nanotube) sheet and Mo_2CT_x–CNT sheet have achieved the capacity of around 420 mAh g^{-1} @ 0.5C and 250 mAh g^{-1} @ 5 A g^{-1}. Also, the flexible clay-like Ti_3C_2 MXene electrode showed better performance in SC of 25 m F cm^{-2} and excellent cyclability of 10000 cycles. Apart from lithium storage, sodium-ion batteries are studied more, where 2D MXene

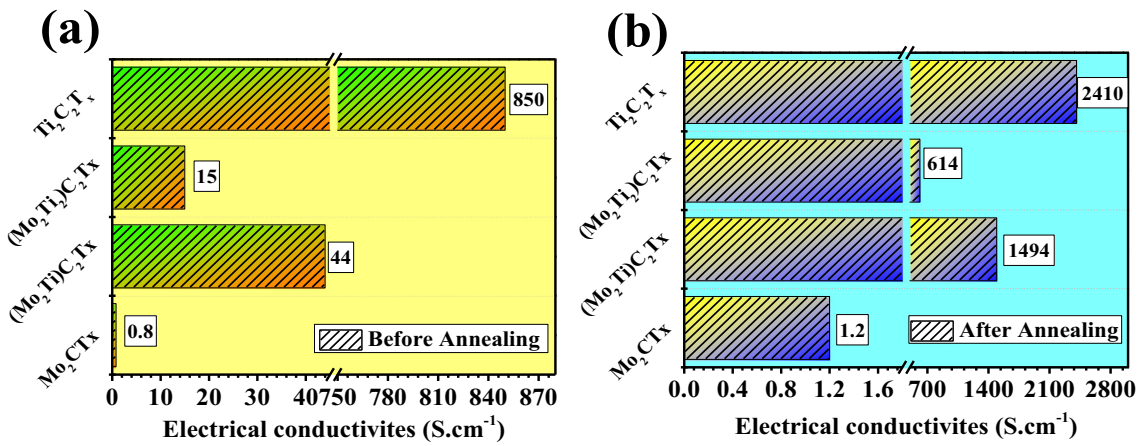

Fig. 9 Electrical conductivities of MXenes before annealing and after annealing

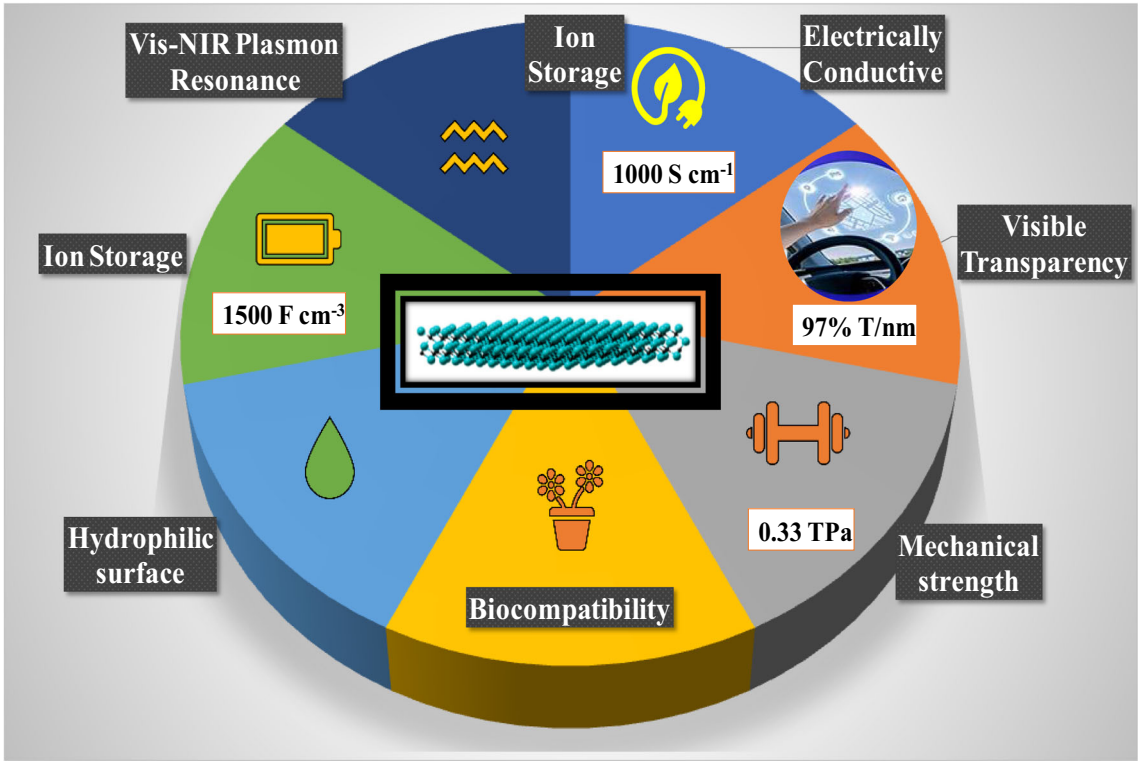

Fig. 10 Properties of titanium carbide MXene ($Ti_3C_2T_x$)

electrodes are evaluated more. Filtration synthesis of porous $Ti_3C_2T_x$/CNT and Mo_2CT_x-CNT paper delivers the anode capacity of 345 mAh cm^{-3} and 700 F cm^{-3} (196 F g^{-1}) in a sodium-ion battery system.

4.1 MXenes as supercapacitor electrodes

ECs usually have higher power densities than LIBs. Nevertheless, energy densities are considerably less. It has a higher energy density but low power density in the battery systems. Similarly, to increase voltage and conductivity while preserving stability, advances in electrolytes are required [55]. It is of utmost importance to know how materials are treated and transferred via electrode-electrolyte interfaces and will have good knowledge of the processes of charge transfer. The ability to synthesize compact, high surface area nanostructured electrodes offers the ability to store various charges at a single site, improving the rate of charge.

More surface features can also provide a reproducible and powerful capacity for energy storage and fast charge and discharge. The design of new materials with special structures designed to withstand capacitive loads efficiently will be spurred with advanced methodologies (computational and analytical) for the production of the material. These methods will also have the molecular insight needed to evaluate the physical and chemical requirements of the electrolytes with higher voltages, improved ion conductivity, and great electrochemical and thermal stability. In this concern, MXenes have been interesting material of SC due to their interesting characteristic property. The high specific surface area with nanosized pores and open channels are very important features for high-performance SCs. For example, Ti_3C_2 MXene-based SC electrodes in aqueous solutions showed excellent cyclic ability and volumetric capacitance of 300–400 F cm^{-3}, which shows three times higher than activated carbon and graphene-based capacitors. Ti_3C_2 MXene clay has a volumetric capacitance of 900 F cm^{-3}, a higher capacity per unit volume than other materials. FL-Ti_3C_2 nanolayers can be tightly mixed with polyvinyl alcohol (PVA) polymers, forming MXene-PVA layered structures. The electrical conductivity of the composite material can be controlled from 4×10^{-4} to 220 S cm^{-1} (by varying the MXene content from 40 to 90%). The composites have a strength of up to 400% higher than flat MXene films and have an increased value of 500 F cm^{-3}. The substitute filtration process for the formulation of MXene-carbon nanomaterial composite film is also being invented. In SC, these composites showed improved performance at high rates. The addition of polymers/carbon nanostructures between some of the layers of MXene allows it simpler for the electrolyte ions to diffuse through the MXenes, the secret to their use in versatile SCs. The high conductivity of composite is highlighted by electrochemical measurements, which is likely due to the small insulation gaps between the MXene flakes and the thin CNFs; vacuum pressing also does not significantly reduce the capacitance of the MXene flakes. Cyclic stability revealed 100% retention of capacity after 10,000 cycles [56].

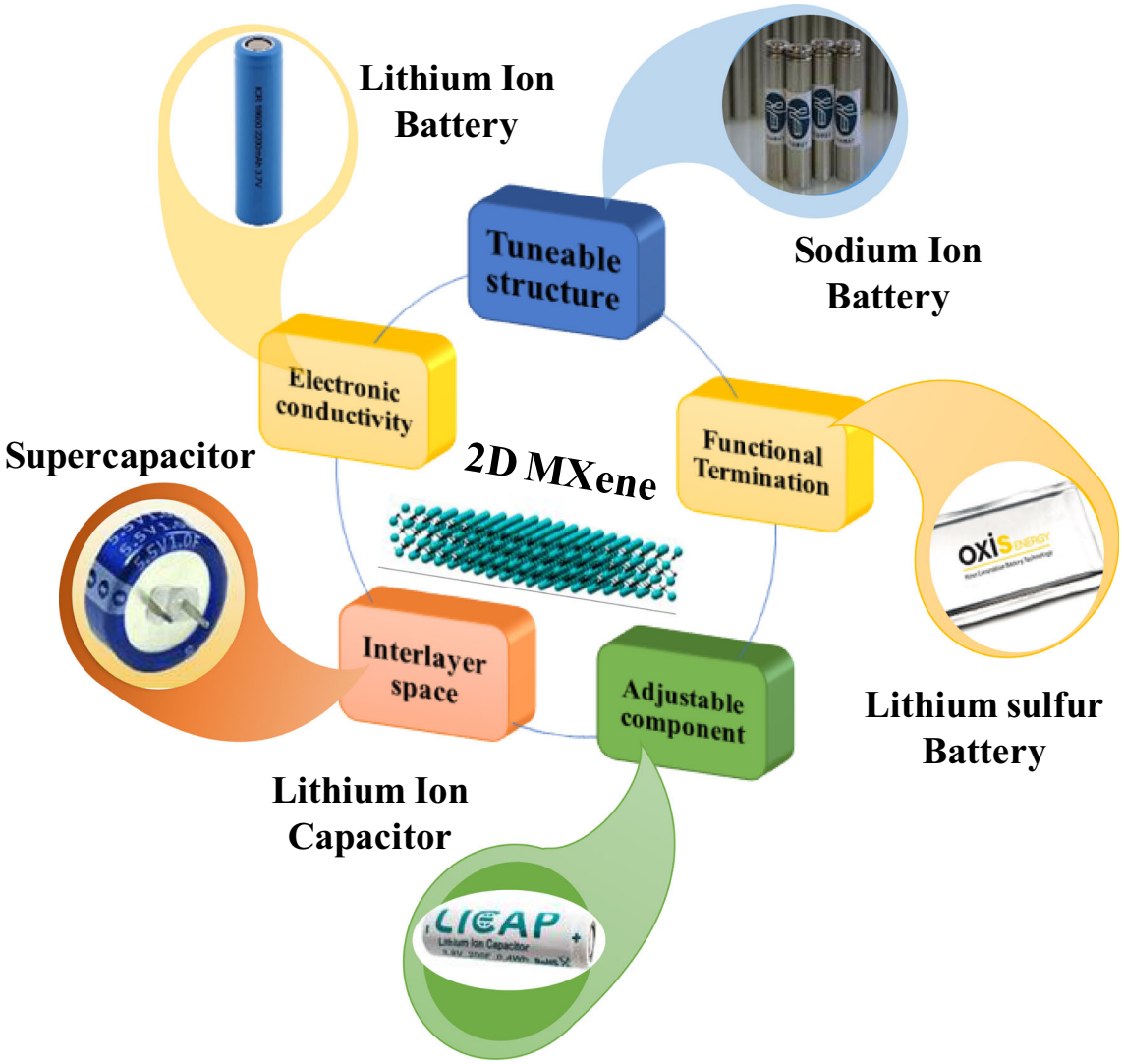

Fig. 11 MXenes and MXene-based nanocomposites as electrical energy storage materials

Figure 12 shows the schematic diagram of the MXene SC. Free-standing $Ti_3C_2T_x$ MXene/carbon nanofiber electrodes are widely used. It is prepared by electrospinning technique, Firstly, $Ti_3C_2T_x$ MXene flakes were dispersed in PAN solution. Then the solution is coated onto the substrate mat followed by carbonizing the fiber networks under an inert atmosphere. The carbonized fiber mat is free standing and free from a binder and additive compounds. Hence, it can act as an self standing electrode for the SC and the addition of composite material to the MXene electrode shows stable and durable performance [57]. So, N_2-doped 2D (N-$Ti_3C_2T_x$) MXene material was found to be a better SC. It was fabricated by post-etch annealing $Ti_3C_2T_x$ in ammonia solution to obtain N-$Ti_3C_2T_x$ [58].

4.2 MXenes based hybrid capacitors

The hybrid capacitor is a type of energy device which combines the properties of both SC and LIBs in a single system and bridges the gap between the two systems. Figure 13 represents the MXene-based hybrid capacitor. Lithium-ion capacitor (LIC) is one of the well-known conventional hybrid capacitors.

MXenes are becoming a promising material for flexible LIC devices. To date, numerous electrode materials were used in LIC systems. Owing to the various Li-ion storage structures, anode materials for LICs are classified into three groups as insertion, conversion, and alloy type and depicted in Fig. 14. The insertion type materials, such as graphite, hard carbon, TiO_2, $Li_4Ti_5O_{12}$ (LTO), and Nb_2O_5, have a stable structure. However, their lower theoretical capacity (< 400 mAh g^{-1}) or high-voltage plateau vs. Li metal made the insertion type material inhibits in maximum use. Second, the alloy-type (Si, Sn, and Sn-based composites) and conversion-type (MoS_2, MnO_2, Fe_3O_4, CoO) materials have a high theoretical capacity (>700 mAh g^{-1}) than insertion type material. However, the strong irreversible strength, large volume change, and slow

Table 1 Comparison of different MXene-based electrodes with their synthesis methodology in various energy storage applications

Materials	Etchant	Synthesis approach	Capacity of anode ($mAhg^{-1}$)	Current density (Ag^{-1})	Retention (%)	No. cycles	Ref.
Li-ion battery	Nb_2CT_x/10%CNT paper	Filtration	420	0.5 C	100	100	[44]
	Mo_2CT_x – CNT paper	Filtration	250, 75	5 Ag^{-1} 10 mAg^{-1}	-	10,000	[46]
	PVP-Sn(IV)-modified Ti_3C_2	Liquid-Phase immersion procedure	544.0	0.5 (1.75C)	94.30	200	[47]
	$Nb_4C_3T_x/Nb_2O_5$	CO_2 oxidation by one-step	208.0	50 mAg^{-1} (0.25 C)	94	400	[48]
NIB	Porous $Ti_3C_2T_x$/CNT	Filtration	345 mAh cm^{-3}	0.1	100	500	[44]
	Mo_2CT_x-CNT paper	Filtration	700 F cm^{-3}	10	100	10,000	[46]
LIC	CTAB-Sn(IV)@Ti_3C_2	Filtration	33 F g^{-1}	2	71.70	4000	[49]
	Nb_2O_5/Nb_2CT_x	One-step CO_2 oxidation	600 m F cm^{-2}	-	-	400	[50]
Hybrid capacitor	Cathode: $LiFePO_4$ Anode: Nb_2CT_x/CNT	-	50–70 Wh L^{-1}	-	-	-	[51]
	Cathode: $LiNi_{1/3}Co_{1/3}Mn_{1/3}O_2$ Anode: Ti_2CT_x	-	160 Wh kg^{-1} @ 220 W kg^{-1}	-	-	-	[52]
Supercapacitor	Clay-like Ti_3C_2 MXene	Filtration	25 mF cm^{-2}	2 $mAcm^{-2}$	92	10,000	[53]
	PPy/$Ti_3C_2T_x$film	Filtration	1000 Fcm^{-3}	5mVs^{-1}	92	25,000	[54]

kinetics of such materials cause severe electrode polarization and decay over cycling. The key problems for the anode are the development of electronic/ion conductivity and the durability of the ring. From this point of view, materials with a well-designed or nano-sized design can effectively minimize the Li^+ diffusion path and improve the transport of electrons.

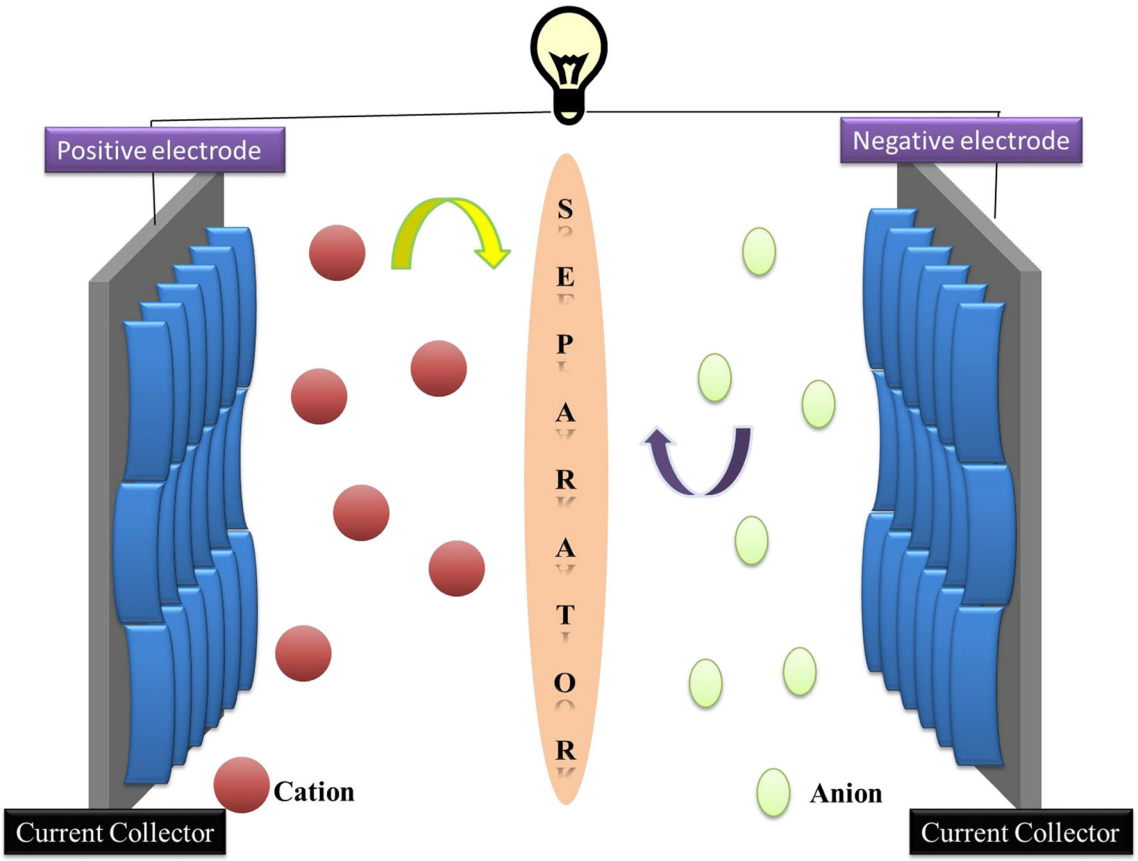

Fig. 12 Schematic representation of MXenes-based supercapacitor electrodes and their electrochemical energy storage mechanism

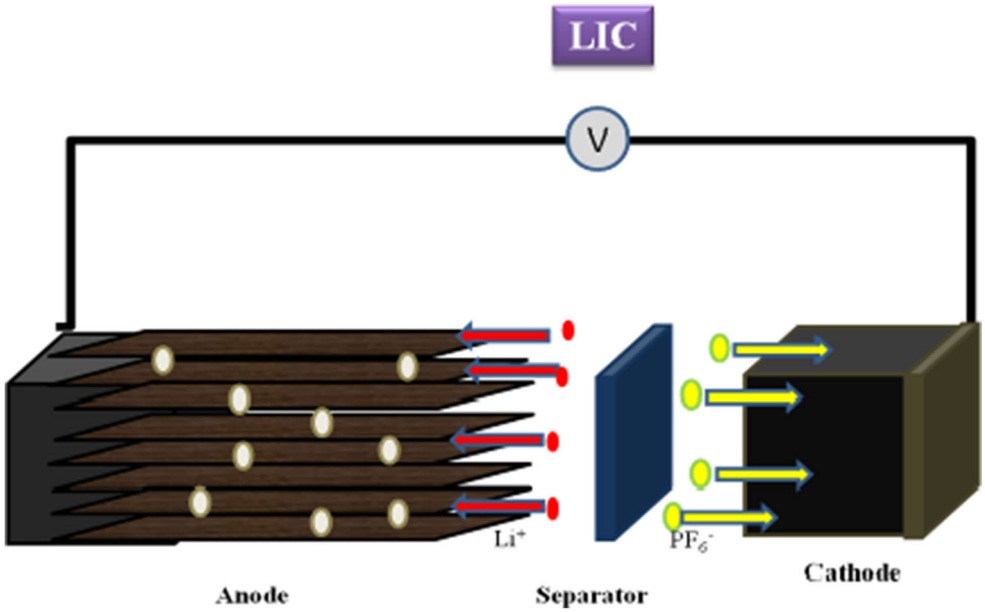

Fig. 13 The principal mechanism of MXene-based hybrid capacitor

The most widely used cathode materials for LIC are graphene, AC, and CNTs. Among different materials, AC has gained much attention due to its specific surface area, ease of synthesis, nontoxicity, and less cost. However, its narrow pore size distribution and pore channels inhibit the diffusion of the electrolyte ion, and comparatively low electron conductivity results in a low power density. As a result, materials with a wide surface area and an acceptable pore size distribution can effectively increase the flexibility and power efficiency of LICs. As a full-cell hybrid electrochemical capacitor, the LIC requires a large-capacity Li^+ reversible intercalation anode to achieve advanced electrochemical energy recovery. MXenes like $Ti_3C_2T_x$, Ti_2CT_x, Nb_2CT_x, and V_2CT_x have a unique, extremely thin, fully accessible layer structure that eases the intercalation/deintercalation kinetics of Li^+. Thus, MXenes demonstrate non-ideal battery behavior but are close to a capacitor that suggests their use in LICs [59, 60]. Moreover, the properties of energy recovery, the stability of MXenes, and the electronic transmission speed are greatly influenced by functional groups (−O, −Cl, −F, −OH,) on the surface of MXene layers.

Table 2 shows that the various MXene electrodes were synthesized by different approaches and etchant to obtain a high-capacity electrode for hybrid LIC application. From the table, it is observed that compared to single MXene material ($Ti_3C_2T_x$ and Ti_2CT_x), composite flexible material ($Ti_3C_2T_x$@Fe_2O_3 and CTAB-Sn(IV)@Ti_3C_2) showed high specific capacity. For example, $Ti_3C_2T_x$ and Ti_2CT_x electrodes showed an anodic performance of 226 F cm^{-3} @ 10 mVs^{-1} and 250 $mAhg^{-1}$ @ 20 mAg^{-1} with a corresponding

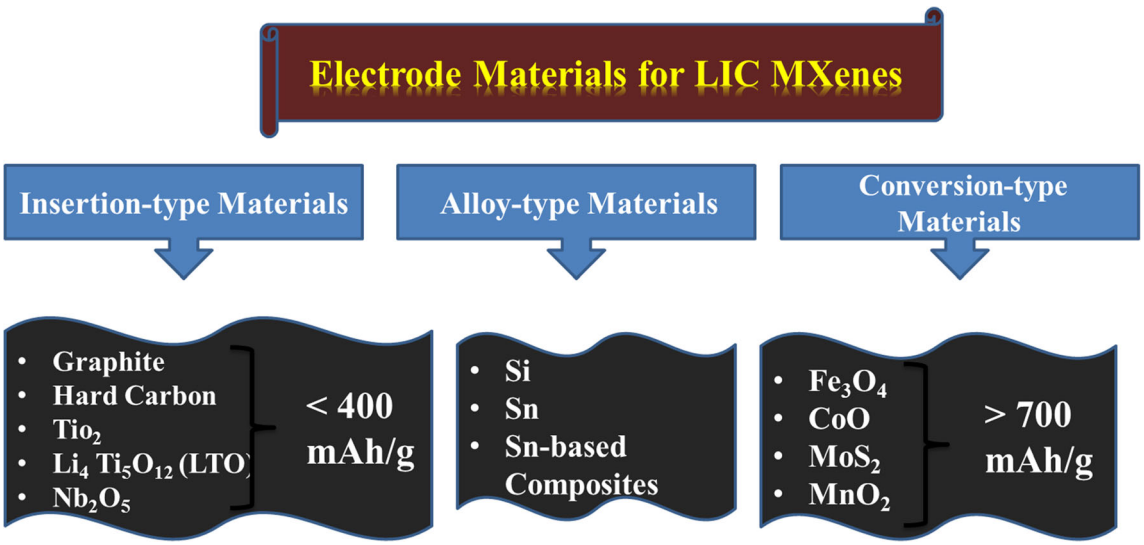

Fig. 14 Various anode materials for Hybrid capacitor

Table 2 MXene-based electrodes for hybrid lithium-ion capacitors

Materials	Etchant	Synthesis approach	Capacity of anode ($mAhg^{-1}$)	Current density (Ag^{-1})	Voltage (V)	E ($Wh\,kg^{-1}$)	P ($W\,kg^{-1}$)	Ref.
$Ti_3C_2T_x$@Fe_2O_3	9M HCL+7.5M LiF, 50% HF, 6M HCl +5M LiF, 9M HCL + 49% HF, 6M HCl+LiF	Surfactant	1180 $mAhg^{-1}$	0.1	0.01–4	216	400	[49]
CTAB-Sn(IV)@Ti_3C_2		Liquid-phase immersion	675	0.1	1–4	105.6	495	[61]
Delaminated $Ti_3C_2T_x$/CNT	9M HCl+3.8M LiF, 9M HCl+1.9M LiF, 12M HCl+3M LiF	TBAOH delamination and filtration	489 mAh g^{-1}	50 mA g^{-1}	1–4	67	258	[52]
Ti_2CT_x	Precursor-Ti_2AlC 10% HF	LiF/HCl Etching	250	0.02	0.4–4.2	160	220	[45]
Nb_2CT_x/CNT	Precursor- Nb_2AlC 50% HF	Amine assisted delamination and filtration	400 $mAhg^{-1}$	0.5C	0–3	325 Fcm^{-3}	-	[62]
Delaminated Nb_2CT_x/CNT	-	TBAOH delamination and filtration	270 mAh g^{-1}	50 mAg^{-1}	0–3	50-70 WhL^{-1}	-	[52]
$Ti_3C_2T_x$	-	LiF/HCl etching	226 F cm^{-3}	10 mVs^{-1}	0–2	20.7μ$Whcm^{-2}$	2.2 $mWcm^{-2}$	[63]

energy density of around 20.7μ Wh cm^{-2} and 160 $Whkg^{-1}$. On the other hand, the composite MXene $Ti_3C_2T_x$@Fe_2O_3 and CTAB-Sn(IV)@Ti_3C_2 electrode showed the maximum anodic capacity of 1180 $mAhg^{-1}$ @ 0.1Ag^{-1} and 675 $mAhg^{-1}$ @ 0.1 Ag^{-1} which contributes to the high energy density value of 216 $Whkg^{-1}$ and 105.6 Wh kg^{-1} for the composite system.

5 MXene-based hybrid supercapacitors as next-generation energy storage device for flexible electronics applications

The innovation of wearable energy storage devices was motivated by the increasing need for wearable electronics. MXenes are regarded as promising flexible electrodes owing to their high conductivity, ultra-high volumetric capacitance, excellent hydrophilic properties, and surface action. In order to help researchers in MXene research, different mechanical, electrical characteristics are correlated for the production of high-quality portable energy storage systems at the core of the design of wearable consumer electronics [54]. Advances in electrodes and electrolytes have given a strong solution to the trade-off between energy and power densities. However, these traditional energy storage systems are usually operationally rigid or non-mobile, limiting their use in flexible electronics. To solve this problem, the development of flexible electrodes with excellent durability and strong electrochemical efficiency is necessary to meet the critical requirements of portable energy storage systems. MXenes, a new class of 2D materials generated by "A" layer insulation from the MAX phases, have gained significant interest in the field of flexible energy storage technologies.

The advantages from outstanding properties such as lateral microscale, atomic layer thickness, and exceptional hydrophilic properties enable MXenes to be easily mounted into flexible film/sheet electrodes using simple vacuum filtration or spray technology. In contrast, MXenes have demonstrated a considerably volumetric capacitance than conventional carbon-based materials, rendering MXenes superior to lightweight, compact electronics. Also, the excellent conductivity of MXenes leads to an exceptionally higher power density than the metal oxides of the semiconductor form, which leads to the fulfillment of the need for the fast-charging functionality of recent consumer electronics. The surface chemistry combined with the high electro-negativity of MXenes will result in the etching of HF acid also makes it possible to fuse MXenes with other nanomaterials to prepare high-performance versatile composite electrodes.

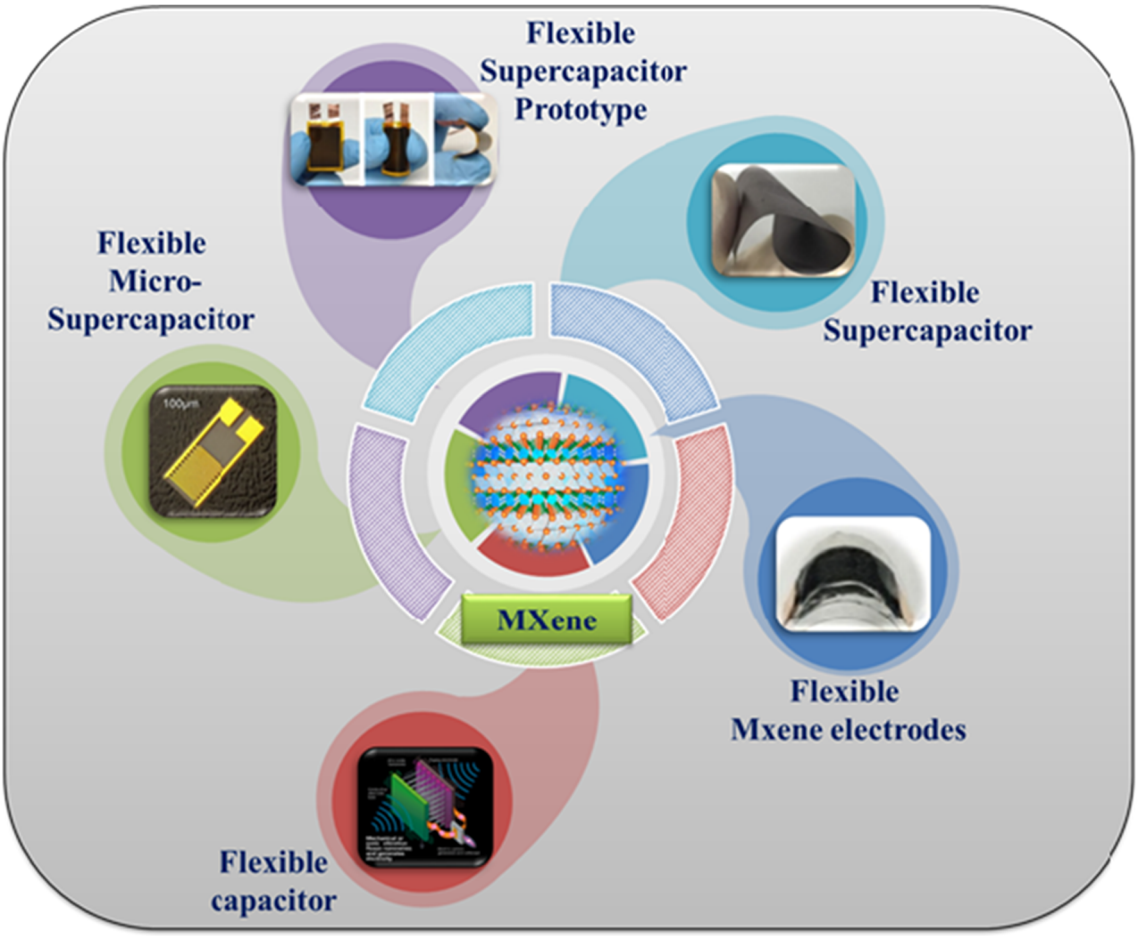

Fig. 15 Flexible MXenes-based supercapacitor

5.1 Fabrication of flexible electronics (role to role fabrication)

The attractive physical, chemical, and biological characteristic and properties of MXene finds a wide utility and also utilized in the application of biosensors, nanogenerators, and electromagnetic interference shielding (EMI) fields. However, 2D MXenes incorporates many characteristics, such as layered composition, metallic conductivity, surface chemistry, and hydrophilicity, which are of huge importance for sensor applications. In particular, the biocompatible, non-toxic, and degradable properties of MXenes are critical for bio- and gas sensors applications. Due to the extraordinary characteristics, MXenes have superior qualities to other extensively reported 2D materials such as graphene and MoS_2. For example, gas such as NO_2^- and H_2O_2 is detected by using Nafion/Hb/MXene $Ti_3C_2T_x$/Glassy carbon electrode (GCE). MXene-based flexible $Ti_3C_2T_x$/graphene oxide (GO) electrodes were fabricated by using inkjet printing technology which exhibited an outstanding performance for H_2O_2 detection.

Furthermore, MXenes are capable of detecting brominated (BrO^{3-}) compounds and volatile organic compounds (VOCs), such as NH_3 and CH_3COCH_3. In addition to detecting gases, MXenes can track minor alterations in stress and strain due to the transmitted layer composition and splendid mechanical properties of the MAX phases. For example, pure $Ti_3C_2T_x$ MXene film possesses high versatility, so it finds an application in highly sensitive piezoresistive sensors [64]. The sensor system operates with the sensing and measuring the value with the external forces which are attributed to the significantly improved interlayer spacing of MXene. This effort and advantage offered by MXenes find an application in mechanical sensors [65]. Also, a versatile strain sensor based on the flexible $Ti_3C_2T_x$ MXene/CNT film was also prepared by layer assembly of the air spray coating process.

Later, a mixture of MXene and PVA hydrogel was developed to demonstrate a high conductive and sensitive strain sensor with outstanding stretchability, for an instant, self-healing capacity, excellent conformability, and adhesiveness to satisfy the complex specifications of wearable electronic devices. These activities show a significant versatility of MXenes in compact sensor systems for environmental measurement and stress detection. In addition, the characteristics of high conductivity and electronegative surface derived from

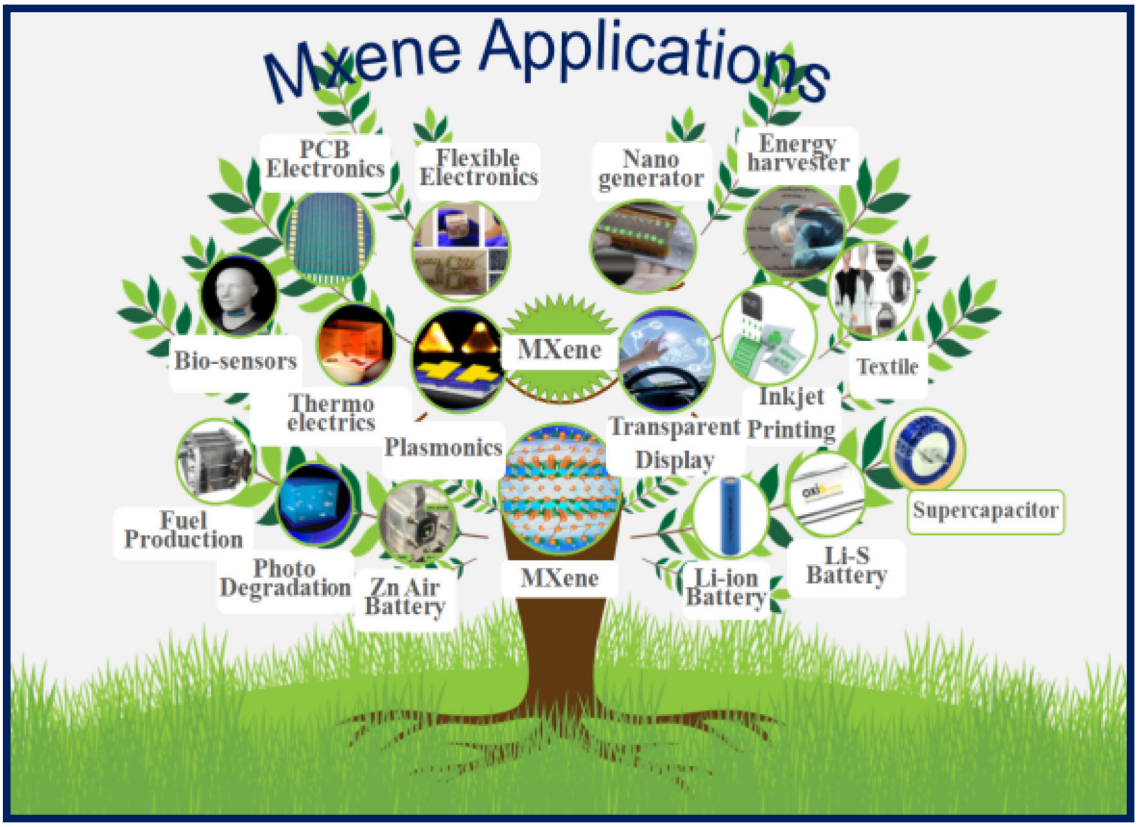

Fig. 16 Potential and versatile applications of MXenes in various fields

negatively charged functional groups also classify metallic MXene as a popular candidate for nanogenerator applications.

For example, $Ti_3C_2T_x$ MXene was successfully synthesized and demonstrated as a self-charging power unit consisting of a compact triboelectric nanogenerator and micro-SCs. Dong et al. have created a versatile nanogenerator based on $Ti_3C_2T_x$ MXene to capture the low power generated by human muscles. Also, the merits of metallic conductivity, active chemical surfaces, and excellent hydrophilicity make it possible for MXenes to play a significant role in the EMI shielding region. Furthermore, Han et al. has also recorded the excellent EMI performance for the $Ti_3C_2T_x$ MXene and reported a value of about 76 dB with a thickness of 1 mm. Later, Shazard et al. has also developed a series of flexible and ultra-thin MXene films based on $Ti_3C_2T_x$, $Mo_2TiC_2T_x$, and $Mo_2Ti_2C_3T_x$ flakes materials and recorded exemplary EMI performance.

5.2 Flexible supercapacitors

MXene films find a desirable application in SC electrodes due to their ultra-high-power density and pseudocapacitive charge storage mechanism. However, the self-discharge of MXene nanosheets has a significant influence on their capacity rate and energy storage. A self-contained and versatile altered nanoporous MXene film is manufactured by inserting $Fe(OH)_3$ nanoparticles with a pore diameter of 3–5 nm. In this process, the nanoparticle is placed into the MXene film by dissolving the $Fe(OH)_3$ nanoparticles than accomplished by carrying outing low calcination temperature at 200°C, which leads to the formation of highly linked nanopore channels that facilitate effective ion transport without sacrificing ultra-high density. As a consequence, the altered nanoporous MXene film poses an attractive volumetric capacitance (1142 F cm^{-3} at 0.5 A g^{-1}) and good rate capability (828 F cm^{-3} at 20 A g^{-1}). But still, the material is possessing a high volumetric capacitance of 749 F cm^{-3} even at a higher active mass loading of 11.2 mg cm^{-2}. Therefore, this flexible and free-standing nanoporous MXene film is a promising electrode material for flexible, portable, and compact storage devices [66]. The various application of MXene-based flexible SC is presented in Fig. 15.

5.3 Applications of MXenes

MXenes are having different structural characteristics, and their versatile nature made them promising material for several potential applications. Among the potential applications, the energy storage and conversion of MXenes were initially identified and extensively reported by several research groups. However, numerous other applications of MXenes are explored in recent years and represented in Fig. 16. For instant,

freestanding $Ti_3C_2T_x$ MXene film exhibits the highest electromagnetic interference shielding ever reported for a synthetic material of comparable thickness. Apart from the energy storage application, MXenes find application in other fields, such as biosensors, flexible electronics, nanogenerators, energy harvester, thermoelectric, inkjet printing, photocatalyst, lubricants, water purifications, reinforcement for composites, and photothermal therapy, which have reported by other research groups [67–74].

6 Summary and outlook

The various synthesis techniques, configurations, and electronic properties of MXenes and MXenes based composites are emphasized and extensively discussed in the present review article. MXenes are generally fabricated by removing "A" layers using HF acid solution from the parent MAX phase. Apart from the toxic HF etching agent, LiF with HCl or H_2SO_4 has also been used as a mild etching agent for the preparation of MXenes. Furthermore, a fluoride-free preparation method plays a vital role in further advances in MXene development. Dimethyl sulfoxide can also be used as an intercalation agent to intercalate into the MXene layers, and hence, large-scale delamination can take place easily and form a single or few layers of MXenes as flexible or free-standing MXene sheets. However, single-layer MXenes show restacking nature due to their electrostatic interaction. Hence, a reliable and stable preparation method is strongly required to obtain flexible and stable MXenes. Apart from the structural characteristics, MXenes are very good electrical conductors, and their surface termination can be easily tunable which plays a major role in energy storage applications. Thus, MXene-based composites have been extensively investigated as an electrode for SC (most investigated MXene: $Ti_3C_2T_x$), LIC, LIB, etc. The free-standing $Ti_3C_2T_x$ electrode shows an excellent volumetric capacitance of around 300–400 F cm^{-3} in various electrolytic mediums. MXenes and their composites have shown excellent and versatile characteristic properties. Unfortunately, single-layer MXene are unstable in oxygen and water environment. On the other hand, MXenes are highly stable in an inert and dry air environment. MXenes are also sensitive to light exposure which may stimulate the oxidation of MXene colloidal solutions. Hence, it is encouraged to store MXene colloids in a refrigerator and an oxygen-free dark environment. Although many breakthroughs of MXenes and MXene-based composites for supercapacitors and hybrid capacitors applications have explored in the past few years, there are still few challenges to address the energy density, power density, and long durability of this material. From the overall observation, it is concluded that MXenes and MXene-based nanocomposites are having very unique properties, but an extensive investigation is required to further demonstrate these materials for realistic applications.

Acknowledgements The authors greatly acknowledge the funding support from the technical research center (TRC) project (Ref. No. AI/1/65/ARCI/2014 (c)) sponsored by the Department of Science and Technology (DST), Government of India, New Delhi, India.

References

1. T. Abbasi, M. Premalatha, S.A. Abbasi, The return to renewables: will it help in global warming control. Renew. Sust. Energ. Rev. **15**, 891–894 (2011)
2. S.O. Amrouche, D. Rekioua, T. Rekiou, S. Bacha, Overview of energy storage in renewable energy systems. J. Hydrog. Energy. **41**, 20914–20927 (2016)
3. H. Shao, P. Narayanasamy, K.M. Razeeb, R.P. Lynch, F.M.F. Rhen, in *Energy Storage Options and Their Environmental Impac*. Electrical storage (2019), pp. 150–183
4. D. Parra, S.A. Norman, G.S. Walker, M. Gillott, Optimum community energy storage for renewable energy and demand load management. Appl. Energy **200**, 358–369 (2017)
5. P. Duffy, C. Fitzpatrick, T. Conway, R.P. Lynch, Energy sources and supply grids – the growing need for storage. Environ. Sci. Technol., 1–41 (2018)
6. P. Alotto, M. Guarnieri, F. Moro, Redox flow batteries for the storage of renewable energy: a review. Renew. Sust. Energ. Rev. **29**, 325–335 (2014)
7. H. Shiyu, Z. Qizhen, S.A. Razium, X. Bin, MXene derivatives for energy storage applications. Sustain. Energy Fuels. **4**, 4988–5004 (2020)
8. A. Ajanovic, Biofuels versus food production: does biofuels production increase food prices. Energy. **36**, 2070–2076 (2010)
9. H.J. Peng, J.Q. Huang, Q. Zhang, A review of flexible lithium–sulfur and analogous alkali metal–chalcogen rechargeable batteries. Chem. Soc. Rev. **46**, 5237–5288 (2017)
10. F. Shi, C. Mang, H. Liu, Y. Dong, Flexible and high-energy-density Zn/MnO_2 batteries enabled by electrochemically exfoliated graphene nanosheets. New J. Chem. **44**, 653–657 (2020)
11. X. Cai, Y. Luo, B. Liu, H.M. Cheng, Preparation of 2D material dispersions and their applications. Chem. Soc. Rev. **47**, 6224–6266 (2018)
12. A.J. Mannix, B. Kiraly, M.C. Hersam, N.P. Guisinger, Synthesis and chemistry of elemental 2D materials. Nat. Rev. Chem. **1**, 01–14 (2017)
13. Y. Gogotsi, B. Anasori, The Rise of MXenes. ACS Nano **13**, 8491–8494 (2019)
14. R. Ronchi, J.T. Arantes, S.F. Santos, Synthesis, structure, properties and applications of MXenes: current status and perspectives. J. Ceram. Int. **45**, 18167–18188 (2019)
15. C. Zhan, W. Sun, Y. Xie, D. Jiang, R. Paul, C. Kent, Computational discovery and design of MXenes for energy applications: status, successes, and opportunities. ACS Appl. Mater. Interfaces **28**, 24885–24905 (2019)
16. Q. Tang, Z. Zhou, Graphene analogous low dimensional materials. Prog. Mater. Sci. **58**, 1244–1315 (2013)
17. M. Ghidiu, M.R. Lukatskaya, M.Q. Zhao, Y. Gogotsi, M.W. Barsoum, Conductive two-dimensional titanium carbide 'clay' with high volumetric capacitance. Nature. **516**, 78–81 (2014)
18. M.R. Lukatskaya, O. Mashtalir, C.E. Ren, Y. Dall'Agnese, P. Rozier, P.L. Taberna, M. Naguib, P. Simon, M.W. Barsoum, Y.

Gogotsi, Cation intercalation and high volumetric capacitance of two-dimensional titanium carbide. Science. **341**, 1502–1505 (2013)
19. B. Ahmed, D.H. Anjum, Y. Gogotsi, H.N. Alshareef, Atomic layer deposition of SnO_2 on MXene for Li-ion battery anodes. Nano Energy **34**, 249–256 (2017)
20. G.E. Mengni, W. Xiaofan, L. Gaiye, L. Chen, Z. Jianfeng, T. Rong, Synthesis of Cr_2AlC from elemental powders with modified pressure less spark plasma sintering. Mater. Sci. **34**, 287–292 (2019)
21. S. Zhao, X. Meng, K. Zhu, F. Du, G. Chen, Y. Wei, Y. Gogotsi, Y. Gao, Li-ion uptake and increase in interlayer spacing of Nb_4C_3 MXene. Energy Storage Mater. **8**, 42–48 (2017)
22. Z. Lin, D. Sun, Q. Huang, J. Yang, M.W. Barsoum, X. Yan, Carbon nanofiber bridged two-dimensional titanium carbide as a superior anode for lithium-ion batteries. J. Mater. Chem. A **3**, 14096–14100 (2015)
23. S. Nyamdelger, T. Ochirkhuyag, D. Sangaa, Odkhuu, First-principles prediction of a two-dimensional vanadium carbide (MXene) as the anode for lithium ion batteries. Phys. Chem. Chem. Phys. **22**, 5807–5818 (2020)
24. B. Ahmed, D.H. Anjum, M.N. Hedhili, Y. Gogotsi, H.N. Alshareef, H_2O_2 assisted room temperature oxidation of Ti_2C MXene for Li-ion battery anodes. Nanoscale. **8**, 7580–7587 (2016)
25. M.Q. Zhao, M. Torelli, C.E. Ren, M. Ghidiu, Z. Ling, B. Anasori, M.W. Barsoum, Y. Gogotsi, 2D titanium carbide and transition metal oxides hybrid electrodes for Li-ion storage. Nano Energy **30**, 603–613 (2016)
26. C.E. Ren, M.Q. Zhao, T. Makaryan, J. Halim, M. Boota, S. Kota, B. Anasori, M.W. Barsoum, Y. Gogotsi, Porous two-dimensional transition metal carbide (MXene) flakes for high-performance Li-ion storage. Chem Electro Chem. **3**, 689–693 (2016)
27. M. Alhabeb, K. Maleski, T.S. Mathis, A. Sarycheva, Selective etching of silicon from Ti_3SiC_2 (MAX) to obtain 2D titanium carbide (MXene). Angew. Chem. Int. **57**, 5444–5448 (2018)
28. M. Naguib, M. Kurtoglu, V. Presser, J. Lu, J. Niu, M. Heon, L. Hultman, Y. Gogotsi, M.W. Barsoum, Two-dimensional nanocrystals produced by exfoliation of Ti_3AlC_2. Adv. Mater. **37**, 4248–4253 (2011)
29. M. Hu, H. Zhang, T. Hu, B. Fan, X. Wang, Z. Li, Emerging 2D MXenes for supercapacitors: status, challenges and prospects. Chem. Soc. Rev. **49**, 6666–6693 (2020)
30. G. Song, R. Kang, L. Guo, Z. Ali, X. Chen, Z. Zhang, C. Yan, C.T. Lin, N. Jiang, J. Yu, Highly flexible few-layer Ti_3C_2MXene/cellulose nanofiber heat-spreader films with enhanced thermal conductivity. New J. Chem. **44**, 7186–7193 (2020)
31. G. Deysher, C.E. Shuck, K. Hantanasirisakul, N.C. Frey, A.C. Foucher, K. Maleski, A. Sarycheva, V.B. Shenoy, E.A. Stach, B. Anasori, Y. Gogotsi, Synthesis of Mo_4VAlC_4 MAX phase and two-dimensional Mo_4VC_4 MXene with five atomic layers of transition metals. ACS Nano **1**, 204–217 (2020)
32. B. Anasori, Y. Xie, M. Beidaghi, J. Lu, B.C. Hosler, L. Hultman, P.R.C. Kent, Y. Gogotsi, M.W. Barsoum, Two-dimensional, ordered, double transition metals carbides (MXenes). ACS Nano **9**, 9507–9516 (2015)
33. M. Magnuson, J. Halim, L. ÅkeNäslund, Chemical bonding in carbide MXene nanosheets. J. Elec. Spec. **224**, 27–32 (2018)
34. Z. Dai, C. Peng, J.H. Chae, K.N. Chiang, G.Z. Chen, Cell voltage versus electrode potential range in aqueous supercapacitors. Sci. Rep. **5**, 9854 (2015)
35. P. Sennu, N. Arun, S. Madhavi, V. Aravindan, Y.S. Lee, All carbon based high energy lithium-ion capacitors from biomass: the role of crystallinity. J. Power Sources **414**, 96–102 (2019)
36. K. Kannan, K.K. Sadasivuni, A.M. Abdullah, B. Kumar, Current trends in MXene-based nanomaterials for energy storage and conversion system: a mini review. Catalysts **10**, 495 (2020)
37. D. Gielen, F. Boshell, D. Saygin, M.D. Bazilian, N. Wagner, R. Gorini, The role of renewable energy in the global energy transformation. Energy Strategy Rev. **24**, 38–50 (2019)
38. M. Ghidu, Ion-exchange and cation solvation reactions in Ti_3C_2 MXene. Chem. Mater. **28**, 13507–13514 (2016)
39. Z. Sen, N. Ravi, Q. Yu, G. Xiaohui, Two-dimensional hybrid nanomaterials derived from MXenes ($Ti_3C_2T_x$) as advanced energy storage and conversion applications. Chin. Chem. Lett. **31**, 947–952 (2020)
40. C. Yang, Y. Tang, Y. Tian, Y. Luo, M.F. Din, X. Yin, W. Que, Flexible Nitrogen-Doped 2D Titanium Carbides (MXene) Films constructed by an ex situ solvothermal method with extraordinary volumetric capacitance. Adv. Energy Mater. **8**, 1802087 (2018)
41. J. Peng, X. Chen, W.J. Ong, X. Zhao, N. Li, Surface and heterointerface engineering of 2D MXenes and their nanocomposites: insights into electro and photocatalysis. Chem. **5**, 18–50 (2018)
42. J. Pang, R.G. Mendes, A. Bachmatiuk, L. Zhao, H.Q. Ta, T. Gemming, H. Liu, Z. Liu, M.H. Rummeli, Applications of 2D MXenes in energy conversion and storage systems. Chem. Soc. Rev. **48**, 72–133 (2019)
43. A. Lipatov, H. Lu, M. Alhabeb, B. Anasori, A. Gruverman, Y. Gogotsi, A. Sinitskii, Elastic properties of 2D $Ti_3C_2T_x$ MXene monolayers and bilayers. Sci. Adv. **4**, 0491 (2018)
44. J. Halim, S. Kota, M.R. Lukatskaya, M. Naguib, M.Q. Zhao, E.J. Moon, J. Pitock, J. Nanda, S.J. May, Y. Gogotsi, M.W. Barsoum, Synthesis and characterization of 2D molybdenum carbide (MXene). Adv. Funct. Mater. **26**, 3118–3127 (2016)
45. O. Mashtalir, M.R. Lukatskaya, M.Q. Zhao, M.W. Barsoum, Y. Gogotsi, Amine-Assisted delamination of Nb_2C MXene for Li-ion energy storage devices. Adv. Mater. **27**, 3501–3506 (2015)
46. J. Luo, X. Tao, J. Zhang, Y. Xia, H. Huang, L. Zhang, Y. Gan, C. Liang, W. Zhang, Sn^{4+} ion decorated highly conductive Ti_3C_2 MXene: promising lithium-ion anodes with enhanced volumetric capacity and cyclic performance. ACS Nano **10**, 2491–2499 (2016)
47. C. Zhang, S.J. Kim, M. Ghidiu, M.Q. Zhao, M.W. Barsoum, V. Nicolosi, Y. Gogotsi, Layered orthorhombic Nb_2O_5@$Nb_4C_3T_x$ and TiO_2@$Ti_3C_2T_x$ hierarchical composites for high performance Li-ion batteries. Adv. Funct. Mater. **26**, 4143–4152 (2016)
48. X. Xie, M.Q. Zhao, B. Anasori, K. Maleski, C.E. Ren, J. Li, B.W. Byles, E. Pomerantseva, G. Wang, Y. Gogotsi, Porous hetero structured MXene/carbon nanotube composite paper with high volumetric capacity for sodium-based energy storage devices. Nano Energy **26**, 513–523 (2016)
49. J. Luo, W. Zhang, H. Yuan, C. Jin, L. Zhang, H. Huang, C. Liang, Y. Xia, J. Zhang, Y. Gan, X. Tao, Pillared structure design of MXene with ultralarge interlayer spacing for high-performance lithium-ion capacitors. ACS Nano, 2459–2469 (2017)
50. C. Zhang, M. Beidaghi, M. Naguib, M.R. Lukatskaya, M.Q. Zhao, B. Dyatkin, K.M. Cook, S.J. Kim, B. Eng, X. Xiao, D. Long, W. Qiao, B. Dunn, Y. Gogotsi, Synthesis and charge storage properties of hierarchical niobium pentoxide/carbon/niobium carbide (MXene) hybrid materials. Chem. Mater. **28**, 3937–3943 (2016)
51. A. Byeon, A.M. Glushenkov, B. Anasori, P. Urbankowski, J. Li, B.W. Byles, B. Blake, K.L. VanAken, S. Kota, E. Pomerantseva, J.W. Lee, Y. Chen, Y. Gogotsi, Lithium-ion capacitors with 2D Nb_2CT_x (MXene) carbon nanotube electrodes. J. Power Sources **326**, 686–694 (2016)
52. S. Kajiyama, L. Szabova, H. Iinuma, A. Sugahara, K. Gotoh, K. Sodeyama, Y. Tateyama, M. Okubo, A. Yamada, Enhanced Li-ion accessibility in MXene titanium carbide by steric chloride termination. Adv. Energy Mater. **7**, 1601873 (2017)
53. N. Kurra, B. Ahmed, Y. Gogotsi, H.N. Alshareef, MXene-on-paper coplanar micro supercapacitors. Adv. Energy Mater. **6**, 1601372 (2016)

54. M. Boota, B. Anasori, C. Voigt, M.Q. Zhao, M.W. Barsoum, Y. Gogotsi, Pseudocapacitive electrodes produced by oxidant-free polymerization of pyrrole between the layers of 2D titanium carbide (MXene). Adv. Mater. **28**, 1517–1522 (2016)
55. H. Kim, B. Anasori, Y. Gogotsi, H.N. Alshareef, Thermoelectric properties of two-dimensional molybdenum-based MXenes. Chem. Mater. **29**, 6472–6479 (2017)
56. S. Levitt, M. Alhabeb, C.B. Hatter, A. Sarycheva, G. Dion, Y. Gogotsi, Electrospun MXene/carbon nanofibers as supercapacitor electrodes. J. Mater. Chem. A **7**, 269–277 (2019)
57. Y. Wen, T.E. Rufford, X. Chen, N. Lid, M. Lyu, L. Dai, L. Wang, Nitrogen-doped $Ti_3C_2T_x$ MXene electrodes for high-performance supercapacitors Author links open overlay panel. J. Nano Eng. **06**, 009 (2017)
58. S. Iqbal, H. Khatoon, A.H. Pandit, S. Ahmad, Recent development of carbon based materials for energy storage devices. Mater. Sci. Technol. **2**, 417–428 (2019)
59. J. Liu, H. Zhang, R. Sun, Y. Liu, Hydrophobic, flexible, and lightweight MXene foams for high-performance electromagnetic-interference shielding. Adv. Mater. **38**, 1702367 (2017)
60. X. Tang, H. Liu, X. Guo, S. Wang, W. Wu, A.K. Mondal, C. Wang, G. Wang, A novel lithium-ion hybrid capacitor based on an aerogel-like MXene wrapped Fe_2O_3 nanosphere anode and a 3D nitrogen sulphur dual-doped porous carbon cathode. Mater. Chem. Front. **2**, 1811–1821 (2018)
61. P. Yu, G. Cao, S. Yi, X. Zhang, C. Li, X. Sun, K. Wang, Y. Ma, Binder-free 2D titanium carbide (MXene)/carbon nanotube composites for high-performance lithium-ion capacitors. Nanoscale. **10**, 5906–5913 (2018)
62. J. Li, N. Kurra, M. Seredych, X. Meng, H. Wang, Y. Gogotsi, Bipolar carbide-carbon high voltage aqueous lithium-ion capacitors. Nano Energy **56**, 151–159 (2019)
63. C.J. Zhang, B. Anasori, A.S. Ascaso, S.H. Park, N. McEvoy, A. Shmeliov, G.S. Duesberg, J.N. Coleman, Y. Gogotsi, V. Nicolosi, 2D molybdenum and vanadium nitrides synthesized by ammoniation of 2D transition metal carbides (MXenes). Nanoscale. **09**, 17722–17730 (2017)
64. X. Zhang, Z. Zhang, Z. Zhou, Review MXene-based materials for electrochemical energy storage. J. Energy. Chem. **08**, 004 (2017)
65. Y. Yang, Z. Cao, P. He, L. Shi, G. Ding, R. Wang, J. Sun, $Ti_3C_2T_x$ MXene-graphene composite films for wearable strain sensors featured with high sensitivity and large range of linear response. Nano Energy **10** (2019)
66. P. Sobolčiak, A. Tanvir, K. Kumar, I. Sadasivuni, Krupa, piezoresistive sensors based on electrospun mats modified by 2D $Ti_3C_2T_x$ MXene. Sensors **19**, 4589 (2019)
67. Z. Fan, Y. Wang, Z. Xie, X. Xu, Y. Yuan, Z. Cheng, Y. Liu, A nanoporous MXene film enables flexible supercapacitors with high energy storage. Nanoscale. **10**, 9642–9652 (2018)
68. S. Uzun, S. Seyedin, A.L. Stoltzfus, A.S. Levitt, M. Alhabeb, M. Anayee, C.J. Strobel, J.M. Razal, G. Dion, Y. Gogotsi, Knittable and Washable multifunctional MXene coated cellulose yarns. Adv. Funct. Mater. **29**, 1905015 (2019)
69. S. Ahn, T.H. Han, K. Maleski, J. Song, Y.H. Kim, M.H. Park, H. Zhou, S. Yoo, Y. Gogotsi, A 2D titanium carbide MXene flexible electrode for high efficiency light emitting diodes. J. Adv. Mater. **32**, 2000919 (2020)
70. A. Jastrzębska, E. Karwowska, T. Wojciechowski, W. Ziemkowska, The atomic structure of Ti_2C and Ti_3C_2 MXenes is responsible for their antibacterial activity toward E.coli bacteria. ACS Nano **10**, 3674–3684 (2016)
71. J. Orangi, F. Hamade,V.A. Davis and, M. Beidaghi, 3D printing of additive-free 2D $Ti_3C_2T_x$ (MXene) ink for fabrication of micro-supercapacitors with ultra-high energy densities, ACS Nano 14, 640–650 (2020)
72. P.S. Sreenilayam, A. Inam, N. Valeria, D. Brabazon, Mxene materials based printed flexible devices for healthcare, biomedical and energy storage applications. Mater, 1369–7021 (2021)
73. X. Yanting, Z. Haitao, H. Haichao, W. Zixing, X. Zhong, Z. Haibo, W. Yuchen, C. Ningjun, Y. Weiqing, High-voltage asymmetric MXene-based on-chip micro-supercapacitors. Nano Energy **74**, 2211–2855 (2020)
74. M. Xin, J. Li, Z. Ma, L. Pan, Y. Shi, MXenes and Their applications in wearable sensors. Front. Chem. **8**, 2296–2646 (2020)